Pleiotropic neuroprotective effects of taxifolin in cerebral amyloid angiopathy

Takayuki Inoue[a], Satoshi Saito[b,c], Masashi Tanaka[a,d,1], Hajime Yamakage[a], Toru Kusakabe[a], Akira Shimatsu[e], Masafumi Ihara[b], and Noriko Satoh-Asahara[a]

[a]Department of Endocrinology, Metabolism, and Hypertension Research, Clinical Research Institute, National Hospital Organization Kyoto Medical Center, Fushimi-ku, 612-8555 Kyoto, Japan; [b]Department of Neurology, National Cerebral and Cardiovascular Center, Suita, 565-8565 Osaka, Japan; [c]Department of Regenerative Medicine and Tissue Engineering, National Cerebral and Cardiovascular Center, Suita, 565-8565 Osaka, Japan; [d]Department of Physical Therapy, Health Science University, Fujikawaguchiko-machi, 401-0380 Yamanashi, Japan; and [e]Clinical Research Institute, National Hospital Organization Kyoto Medical Center, Fushimi-ku, 612-8555 Kyoto, Japan

Edited by Lawrence Steinman, Stanford University School of Medicine, Stanford, CA, and approved April 9, 2019 (received for review January 28, 2019)

Cerebral amyloid angiopathy (CAA) results from amyloid-β deposition in the cerebrovasculature. It is frequently accompanied by Alzheimer's disease and causes dementia. We recently demonstrated that in a mouse model of CAA, taxifolin improved cerebral blood flow, promoted amyloid-β removal from the brain, and prevented cognitive dysfunction when administered orally. Here we showed that taxifolin inhibited the intracerebral production of amyloid-β through suppressing the ApoE–ERK1/2–amyloid-β precursor protein axis, despite the low permeability of the blood–brain barrier to taxifolin. Higher expression levels of triggering receptor expressed on myeloid cell 2 (TREM2) were associated with the exacerbation of inflammation in the brain. Taxifolin suppressed inflammation, alleviating the accumulation of TREM2-expressing cells in the brain. It also mitigated glutamate levels and oxidative tissue damage and reduced brain levels of active caspases, indicative of apoptotic cell death. Thus, the oral administration of taxifolin had intracerebral pleiotropic neuroprotective effects on CAA through suppressing amyloid-β production and beneficially modulating proinflammatory microglial phenotypes.

cerebral amyloid angiopathy | neuroprotection | taxifolin | triggering receptor expressed on myeloid cell 2

Cerebral amyloid angiopathy (CAA) is a cerebral small vessel disease, characterized pathologically by the deposition of amyloid-β in the cerebrovasculature (1–3). CAA causes intracerebral hemorrhage and cognitive impairment in elderly people and is often accompanied by Alzheimer's disease (AD) and vascular dementia (1–3). There is therefore an urgent need for predictive markers and effective treatments for CAA.

Taxifolin, also known as dihydroquercetin, is a natural bioactive flavonoid found in various foods and herbs (4). The safety profile of taxifolin has been established (5, 6), and taxifolin has been reported to exhibit various pharmacological effects, including antioxidative, antinitrosative, and antiinflammatory effects (7, 8). In vitro studies have demonstrated that taxifolin had an inhibitory effect on the aggregation of the 42-residue amyloid-β protein (amyloid-β_{1-42}) involved in the pathogenesis of AD (9, 10), suggesting that taxifolin may have the potential to help prevent or treat AD. However, the ability of taxifolin to cross the blood–brain barrier (BBB) is limited and has been assumed to be too low to prevent intracerebral amyloid-β aggregation (3, 4).

We recently showed that in a mouse model of CAA, taxifolin administered orally improved cerebrovascular and cognitive function (3). In vitro, taxifolin inhibited the aggregation of amyloid-β_{1-40}, a major component of vascular amyloid-β deposits; in vivo, it reduced the levels of amyloid-β oligomers in the brain, with a concomitant increase in the levels of amyloid-β_{1-40} in circulation (3). This suggested that taxifolin could facilitate amyloid-β clearance from the brain, perhaps through the intramural periarterial drainage (IPAD) system, a vascular-mediated amyloid-β elimination system. This could potentially maintain vascular integrity, alleviate amyloid-β deposits, and prevent cognitive dysfunction (3, 11). However, the intracerebral mechanisms underlying the potential therapeutic effects of taxifolin for CAA have not been comprehensively elucidated.

Triggering receptor expressed on myeloid cell 2 (TREM2) is a transmembrane protein expressed exclusively on microglia in the brain. Microglia are the main cell involved in the innate immune system in the brain, and they also modulate neuroinflammatory states (12, 13). TREM2 releases its soluble ectodomain, soluble TREM2 (sTREM2), into the extracellular space via cleavage by proteases such as ADAM10 (14). Significant associations have been reported between TREM2 variants and an increased risk for neurodegenerative diseases, including AD (12, 13). TREM2 has been demonstrated to have antiinflammatory effects, mainly based on in vitro analyses; however, there is accumulating evidence suggesting that TREM2 and TREM2-expressing microglia may be implicated in the pathology of neuroinflammation and concomitant neurodegeneration in disease settings, characterized by in vivo mouse models such as those for AD, tauopathy, and diet-induced obesity (13, 15–18). In addition, it was recently reported that sTREM2 was implicated in chronic inflammation through promotion of the survival or activation of macrophages and microglia (19, 20). Further, it has been suggested that elevated sTREM2 levels in human cerebrospinal fluid reflect microglial activation and might provide a novel clinical marker for neurodegenerative diseases (21). Recently, we reported that serum sTREM2 levels may also have utility as a

Significance

Cerebrovascular amyloid-β deposition is highly implicated in the pathogenesis of cerebral amyloid angiopathy (CAA), one of the major causes of dementia. We previously showed that orally administered taxifolin, a natural bioactive flavonoid, enhanced the clearance of amyloid-β, improved cerebral blood flow, and suppressed cognitive decline in a mouse model of CAA. Here we investigate the in vivo effects of taxifolin on intracerebral factors associated with neuronal injury in these mice. We find that orally administered taxifolin may have neuroprotective effects through suppressing intracerebral amyloid-β production, neuroinflammation, and oxidative tissue damage, despite the low permeability of the blood–brain barrier to taxifolin. Our findings suggest taxifolin as a potential target for clinical applications to prevent/treat CAA.

Author contributions: M.T. designed research; T.I. and S.S. performed research; T.I., S.S., M.T., H.Y., T.K., A.S., M.I., and N.S.-A. analyzed data; and T.I., S.S., M.T., M.I., and N.S.-A. wrote the paper.

The authors declare no conflict of interest.

This article is a PNAS Direct Submission.

Published under the PNAS license.

[1]To whom correspondence should be addressed. Email: masashi.7.tanaka@gmail.com.

This article contains supporting information online at www.pnas.org/lookup/suppl/doi:10.1073/pnas.1901659116/-/DCSupplemental.

Published online April 29, 2019.

novel marker for cognitive impairment in Japanese patients with nonobese type 2 diabetes (22) and in the general elderly Japanese population (23). However, the pathophysiological significance of TREM2 in CAA and the effects of taxifolin on microglial phenotypes have not been clarified.

In the present study, we comprehensively investigated the effects of taxifolin on factors potentially implicated in neuronal injury, such as amyloid-β and inflammatory mediators, in a mouse model of CAA, focusing on the potential pathological significance of TREM2. The results provide molecular evidence for the beneficial effects of taxifolin on suppressing cognitive dysfunction in CAA.

Results

Taxifolin Exhibited Protective Effects on the Brain Cells of CAA Model Mice. All of the experiments used a mouse model of CAA based on Tg-SwDI mice (3). These were randomly divided into control and taxifolin groups and fed either standard chow or chow containing taxifolin for 7–13 mo. Hippocampus and cortex tissues were analyzed separately.

To clarify the mechanisms underlying taxifolin's effects in suppressing cognitive decline in CAA model mice, we first investigated whether taxifolin protected their hippocampus and cortex cells from cell death because activation of caspase-mediated apoptotic pathways has previously been suggested in CAA (24). In the hippocampus, taxifolin suppressed the formation of the active apoptotic initiator caspase-9 to a near significant level compared with control ($P = 0.07$; Fig. 1*A*) and significantly suppressed the active apoptotic effectors caspases 3 and 7 (25) ($P < 0.05$; Fig. 1 *B* and *C*). Extracellular deposition of amyloid-β and the intraneuronal accumulation of hyperphosphorylated tau (pTau) induce apoptotic cell death in the brain (26), and Tg-SwDI mice show amyloid-β accumulation (27) but no remarkable tau pathology (28). We therefore examined the effects of taxifolin on these factors. In the hippocampus, taxifolin significantly reduced the amount of amyloid-$\beta_{1–40}$ (the major component of vascular amyloid-β deposits) in line with

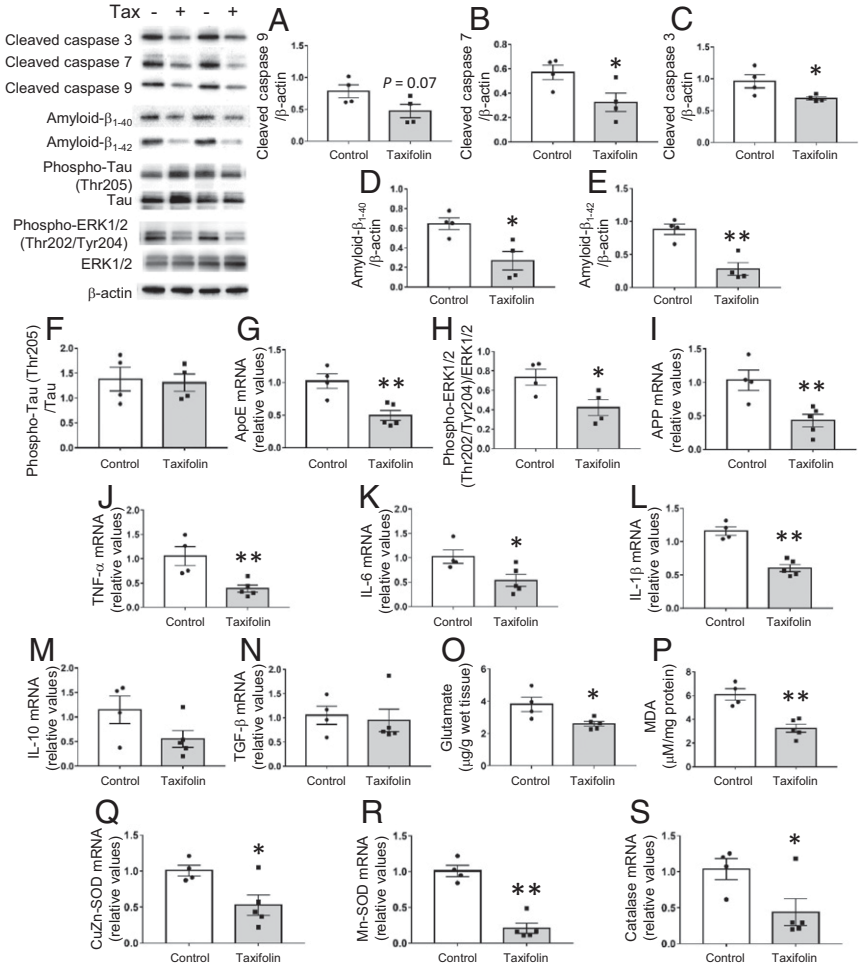

Fig. 1. Protective effects of taxifolin on brain cells in the hippocampus of Tg-SwDI mice. Each histogram compares values for the same 14-mo-old Tg-SwDI mice that received either the control diet ($n = 4$) or taxifolin-containing chow ($n = 5$) for 13 mo. Relative amounts were analyzed by Western blot and densitometry, and mRNA expression levels were obtained by quantitative RT-PCR and normalized to those of GAPDH. *Upper Left* shows representative immunoblots. (*A–C*) Activation levels of the apoptosis-related caspases cleaved caspase-9 (*A*), cleaved caspase-7 (*B*), and cleaved caspase-3 (*C*) relative to β-actin. (*D–F*) Accumulation of amyloid-β and hyperphosphorylated tau proteins in the hippocampal tissue: amyloid-$\beta_{1–40}$ (*D*) and amyloid-$\beta_{1–42}$ (*E*) relative to β-actin and phospho-tau (Thr205) relative to total tau (*F*). (*G–I*) Activation levels of pathways involved in amyloid-β production in the hippocampal tissue: mRNA levels of ApoE (*G*) and APP (*I*) and the amount of phospho-ERK1/2 (Thr202/Tyr204) relative to total ERK (*H*). (*J–N*) Expression levels of proinflammatory and antiinflammatory cytokines in the hippocampal tissue: mRNA levels of TNF-α (*J*), IL-6 (*K*), IL-1β (*L*), IL-10 (*M*), and TGF-β (*N*). (*O*) Glutamate levels in the hippocampal tissue. (*P*) Levels of free lipid peroxides, MDA, in the hippocampal tissue. (*Q–S*) Expression levels of oxidative stress-responsive genes in the hippocampal tissue: mRNA levels of CuZn-SOD (*Q*), Mn-SOD (*R*), and catalase (*S*). Data are expressed as mean ± SEM (control, $n = 4$; taxifolin, $n = 5$). *P* values were determined by Student's *t* test. $^*P < 0.05$; $^{**}P < 0.01$.

our previous report (3) ($P < 0.05$; Fig. 1*D*). Taxifolin also significantly reduced the amount of amyloid-$\beta_{1–42}$, which accumulates in senile plaques ($P < 0.01$; Fig. 1*E*), but it did not reduce the amount of pTau ($P > 0.05$; Fig. 1*F*). Similar results were obtained in cortex tissue of these mice (*SI Appendix*, Fig. S1 *A–F*). Thus, taxifolin exhibits protective effects on brain cells, potentially through reducing levels of both amyloid-$\beta_{1–40}$ and amyloid-$\beta_{1–42}$ in the brain.

We next examined whether taxifolin was involved in attenuating amyloid-β production and other types of cytotoxic mediators in the brain. In the hippocampus, the taxifolin group mice showed a significant reduction compared with the control group in the gene expression levels of ApoE, which enhances the transcription of amyloid-β precursor protein (APP) and the secretion of amyloid-β through ERK1/2 MAPK activation (29) ($P < 0.01$; Fig. 1*G*). In addition, the phosphorylation levels of ERK1/2 ($P < 0.05$; Fig. 1*H*) and the expression levels of APP ($P < 0.01$; Fig. 1*I*) were significantly reduced in the taxifolin group. Furthermore, the brains of Tg-SwDI mice are reported to be in a proinflammatory state compared with wild-type mice (30), and taxifolin treatment led to significantly lower gene expression levels compared with control of the proinflammatory cytokines tumor necrosis factor (TNF)-α ($P < 0.01$; Fig. 1*J*), interleukin (IL)-6 ($P < 0.05$; Fig. 1*K*), and IL-1β ($P < 0.01$; Fig. 1*L*), without substantial effects on levels of the antiinflammatory cytokines IL-10 and TGF-β (Fig. 1 *M* and *N*). Similar results were obtained in the cortex (*SI Appendix*, Fig. S1 *G–N*).

Activated microglia release glutamate, which induces excitotoxic neuronal death; this is potentiated by reactive oxygen species causing oxidative damage to cellular components (31, 32). Additionally, the levels of reactive oxygen species are elevated in the brain of amyloid-β–overexpressing mice compared with wild-type mice (33, 34). Taxifolin treatment resulted in significant ($P < 0.05$) and near-significant ($P = 0.07$) decreases in glutamate levels in hippocampus and cortex tissues, respectively, compared with control (Fig. 1*O* and *SI Appendix*, Fig. S1*O*), as well as significant reductions in the level of cerebral lipid peroxidation, a marker for oxidative tissue damage in the brain (35) (hippocampus, $P < 0.01$, Fig. 1*P*; cortex, $P < 0.05$, *SI Appendix*, Fig. S1*P*). Furthermore, the expression levels of oxidative stress-responsive genes remained significantly lower in the hippocampus tissue from the taxifolin group mice (Fig. 1 *Q–S*). Similar results, except for the level of Mn-SOD expression, were obtained in the cortex (*SI Appendix*, Fig. S1 *Q–S*).

There were no significant differences between the control and taxifolin group mice in anthropometric or metabolic parameters (*SI Appendix*, Fig. S2 *A–H*).

Taxifolin Contributed to the Integrity of the Lymphatic Vasculature. We previously showed that taxifolin prevented the aggregation of amyloid-β and discussed the possibility that taxifolin could stimulate IPAD and contribute to mediating the clearance of amyloid-β (3). We therefore examined whether taxifolin treatment also affected the blood vasculature and/or components, which might be related to drainage function. In both the hippocampus and the cortex, there was no significant difference between the control and taxifolin group mice in the expression levels of claudin-5, one of the tight-junction components expressed on cerebrovascular endothelial cells (36) (Fig. 2*A* and *SI Appendix*, Fig. S3*A*). Conversely, the hippocampal and cortical expression levels of hypoxia-responsive genes were significantly lower in the taxifolin group (Fig. 2 *B–D* and *SI Appendix*, Fig. S3 *B–D*), with the exception of those for vascular endothelial growth factor (VEGF) (Fig. 2*E* and *SI Appendix*, Fig. S3*E*). This supported our recent findings that taxifolin improved cerebral blood flow in Tg-SwDI mice (3).

A previous study reported that meningeal lymphatic vessels were involved in cerebrospinal fluid drainage into the periphery (37). We therefore investigated markers of lymphatic endothelial cells (37, 38). In the hippocampus, the expression levels of

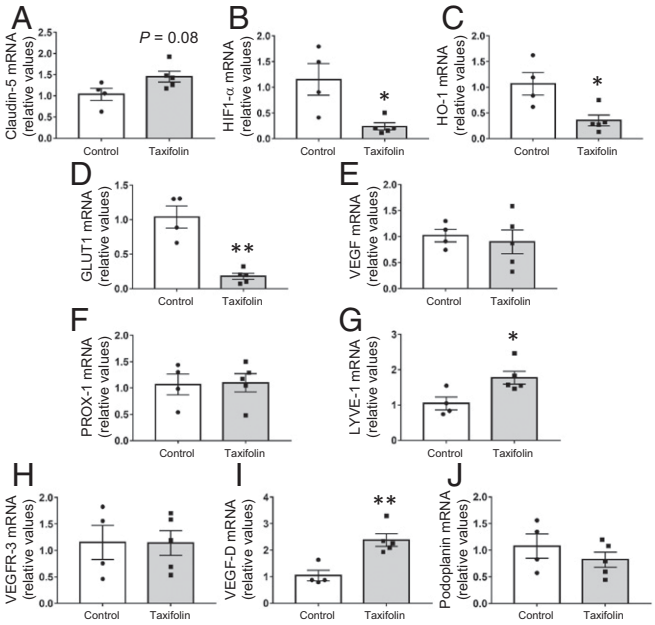

Fig. 2. Effects of taxifolin on expression levels of blood and lymphatic vasculature-related or hypoxia-responsive genes in the hippocampus of Tg-SwDI mice. Each histogram compares values for the same 14-mo-old Tg-SwDI mice that received either the control diet ($n = 4$) or taxifolin-containing chow ($n = 5$) for 13 mo. mRNA levels were analyzed by quantitative RT-PCR and normalized to GAPDH. (*A*) Expression levels of tight-junction–related cerebrovascular endothelial marker, claudin-5, in the hippocampal tissue. (*B–E*) mRNA expression levels of hypoxia-responsive genes in the hippocampal tissue: HIF-1α (*B*), HO-1 (*C*), GLUT1 (*D*), and VEGF (*E*). (*F–J*) Gene mRNA expression levels of markers for lymphatic endothelial cells in the hippocampal tissue: PROX-1 (*F*), LYVE-1 (*G*), VEGFR-3 (*H*), VEGF-D (*I*), and podoplanin (*J*). Data are expressed as mean ± SEM (control, $n = 4$; taxifolin, $n = 5$). *P* values were determined by Student's *t* test. $^*P < 0.05$; $^{**}P < 0.01$.

PROX-1, VEGFR-3, and podoplanin did not differ significantly between the taxifolin and control groups, but the levels of LYVE-1 and VEGF-D were significantly elevated in the taxifolin group ($P < 0.05$ and $P < 0.01$, respectively; Fig. 2 *F–J*). In the cortex, there were no significant differences between the taxifolin and control groups in the expression levels of these markers (*SI Appendix*, Fig. S3 *F–J*). LYVE-1 and VEGF-D play important roles in lymphangiogenesis (38, 39); these findings imply that taxifolin contributes to the integrity of the lymphatic vasculature in Tg-SwDI mice.

Taxifolin Exerted No Remarkable Effect on Levels of Endoplasmic Reticulum Stress Markers and Neurotrophic Growth Factors. The accumulation of protein aggregates induces a stress reaction of the endoplasmic reticulum (ER), and hyperactivation of the ER has been implicated in various neurodegenerative diseases (40). We found no significant difference in ER stress markers between the control and taxifolin group mice (*SI Appendix*, Fig. S4 *A–J*). There was also no substantial difference between the groups in the expression levels in the hippocampus and cortex of BDNF and GDNF, neurotrophic growth factors involved in neuroprotection and adult neurogenesis (41) (*SI Appendix*, Fig. S5 *A–D*).

Taxifolin Suppressed the Accumulation of Activated Microglia in the Hippocampus and Cortex. As described earlier, taxifolin treatment reduced the levels of proinflammatory cytokines, glutamate, and oxidative tissue damage in the brain. Furthermore, microglia are reported to be activated in the brain of Tg-SwDI mice compared with wild-type mice (30). We therefore examined whether taxifolin influenced the accumulation of activated microglia. Immunohistochemical analyses revealed that cells positive for Iba-1, a microglial

activation marker (42), were significantly decreased in the taxifolin group compared with the control group in both the hippocampus and cortex (Fig. 3 *A–D*). Similar results were obtained for TNF-α–positive cells (Fig. 3 *E–H*). In addition, TREM2-positive cells were decreased in the taxifolin group compared with the control group (Fig. 3 *I–L*).

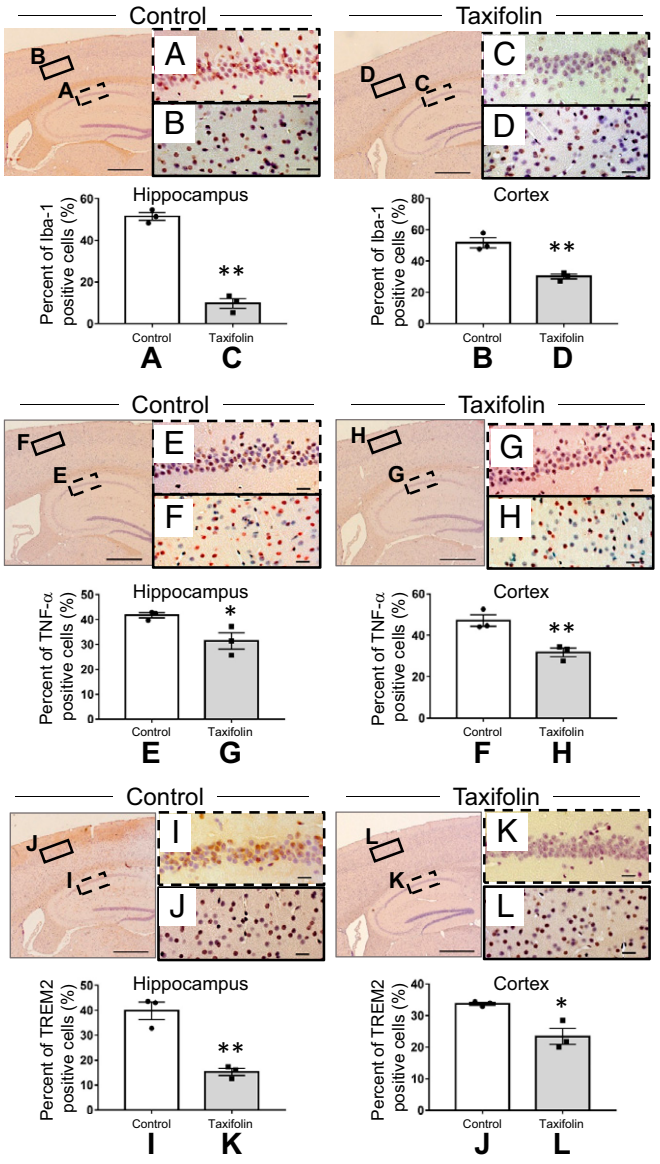

Fig. 3. Effects of taxifolin on the accumulation of cells expressing Iba-1, TNF-α, or TREM2 in the hippocampus or cortex of Tg-SwDI mice. The histograms and representative images are for Tg-SwDI mice that received the control diet (control group, $n = 3$) or chow containing taxifolin (taxifolin group, $n = 3$) for 7 mo. The various cells were detected immunohistochemically, and the total cells were visualized by counterstaining with hematoxylin. Representative images are shown for the control group (*Left*) and taxifolin group (*Right*). [Scale bars, 500 μm for the low-power field (*Left*) and 20 μm for the high-power field (*Right*).] The proportion of positive cells was obtained by dividing the number of immunohistochemically positive cells by the total number of cells. (*A–D*) Immunohistochemical analyses of Iba-1–expressing cells in the hippocampus (*A* and *C*) and cortex (*B* and *D*) of the control group (*A* and *B*) and taxifolin group (*C* and *D*). (*E–H*) Immunohistochemical analyses of TNF-α–positive cells in the hippocampus (*E* and *G*) and cortex (*F* and *H*) of the control group (*E* and *F*) and taxifolin group (*G* and *H*) ($n = 3$). (*I–L*) Immunohistochemical analyses of cells positive for TREM2 in the hippocampus (*I* and *K*) and cortex (*J* and *L*) of the control group (*I* and *J*) and taxifolin group (*K* and *L*). Data are expressed as mean ± SEM (control, $n = 3$; taxifolin, $n = 3$). *P* values were determined by Student's *t* test. $^{*}P < 0.05$; $^{**}P < 0.01$.

Taxifolin Beneficially Affected the Proinflammatory Phenotypes of Microglia. We next examined the effects of taxifolin on inflammation in the brain in more detail. Consistent with the immunohistochemical analyses just described, expression levels of Iba-1 were significantly reduced in the hippocampus in the taxifolin group ($P < 0.05$; Fig. 4*A*). Furthermore, taxifolin significantly reduced the expression levels of TREM2 and ADAM10 ($P < 0.05$ and $P < 0.01$, respectively; Fig. 4 *B* and *C*) and reduced sTREM2 levels to a near-significant extent ($P = 0.05$; Fig. 4*D*). In addition, taxifolin treatment significantly reduced the activation of p38 MAPK, a key signaling molecule involved in the production of inflammatory mediators (43), through reducing levels of phosphorylation at Thr180/Tyr182 ($P < 0.01$; Fig. 4*E*). Taxifolin treatment also resulted in the inhibition of phosphorylation of the stress-associated transcription factor NF-κB subunit p65 at Ser536, which is involved in enhancing its activity (44) ($P < 0.01$; Fig. 4*F*). Similar results were obtained for the cortex, except that the decrease in TREM2 expression was only near significant ($P = 0.08$; *SI Appendix*, Fig. S6 *A–F*). These results suggest that taxifolin contributes to the alleviation of proinflammatory signaling in the brain, where microglia play a major role in the innate immune response.

We next investigated whether taxifolin influenced epigenetic modifications involved in regulating gene expression. DNA methylation is a main contributor to stabilizing gene expression states (45); we therefore analyzed the expression levels of three major mammalian DNA methyltransferases (DNMTs): DNMT1, DNMT3a, and DNMT3b. The function of DNMT1 is to maintain DNA methylation, whereas DNMT3a and DNMT3b are responsible for de novo DNA methylation (46). Although taxifolin treatment affected the expression levels of the DNMTs in the hippocampus and cortex (*SI Appendix*, Fig. S7 *A–F*), global DNA methylation levels did not differ significantly between the taxifolin and control groups (*SI Appendix*, Fig. S7 *G* and *H*).

Recent studies have highlighted the emerging pathological roles of TREM2 and TREM2-expressing microglia in in vivo disease settings (13, 17), although the pathophysiological significance of TREM2 and TREM2-expressing microglia in CAA remains unknown in the clinical setting. To investigate the characteristics of TREM2-expressing microglia and the in vivo effects of taxifolin on these cells, we examined associations between expression levels of TREM2 and those of Iba-1, ADAM10, and cytotoxic mediators (Fig. 4 *G–M*). In the hippocampus, the expression level of TREM2 exhibited significant positive correlations with the levels of ADAM10 [correlation coefficient (r) = 0.8269, $P < 0.01$], TNF-α ($r = 0.7454$, $P < 0.05$), and IL-1β ($r = 0.8294$, $P < 0.01$) (Fig. 4 *H*, *I*, and *K*), but there was not with levels of glutamate (Fig. 4*L*) or lipid peroxidation (Fig. 4*M*). In the cortex, the expression levels of TREM2 were positively correlated with the levels of Iba-1 ($r = 0.9300$, $P < 0.01$), ADAM10 ($r = 0.8249$, $P < 0.01$), TNF-α ($r = 0.7333$, $P < 0.05$), and IL-6 ($r = 0.9138$, $P < 0.01$) (*SI Appendix*, Fig. S6 *G–M*). These results imply that microglia with higher expression levels of TREM2 show a more deleterious proinflammatory phenotype and that taxifolin has beneficial effects on the proinflammatory axis of TREM2-expressing microglia.

Discussion

This study shows that despite its limited ability to cross the BBB, taxifolin exhibited in vivo pleiotropic beneficial effects on intracerebral profiles in a mouse model of CAA when administered orally over several months. Taxifolin treatment reduced amyloid-β accumulation, suppressed microglial activation, and

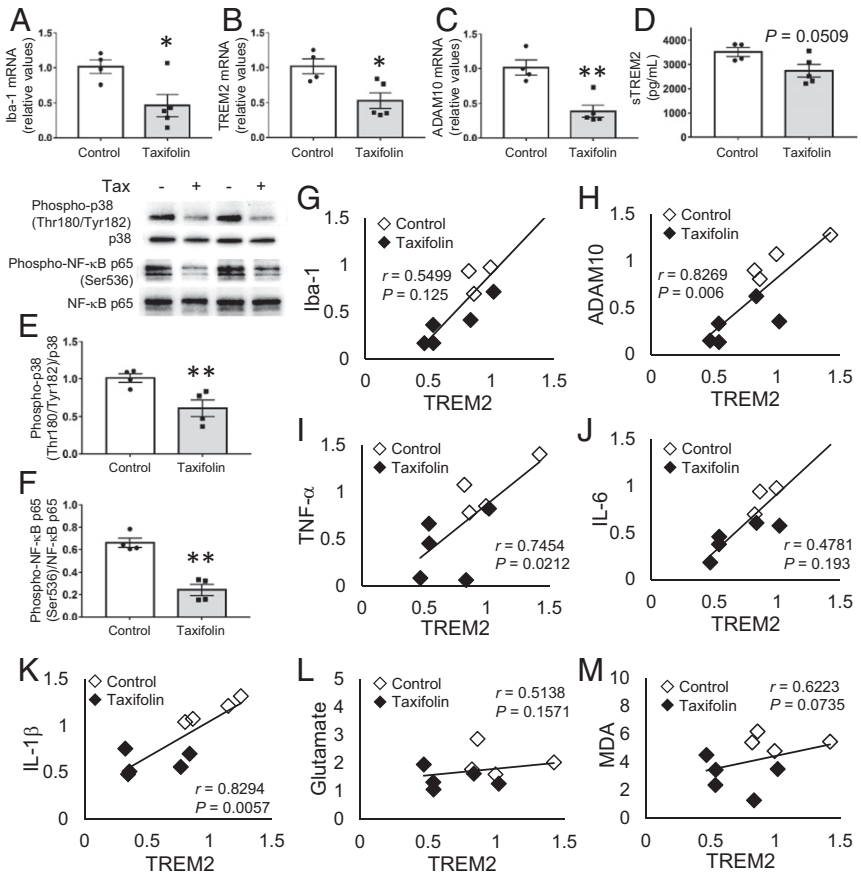

Fig. 4. Beneficial effects of taxifolin on proinflammatory phenotypes of microglia in the hippocampus of Tg-SwDI mice. The histograms and graphs show results for the hippocampal tissue of 14-wk-old Tg-SwDI mice that received either the control diet ($n = 4$) or chow containing taxifolin ($n = 5$) for 13 mo. mRNA expression levels were measured by quantitative RT-PCR and normalized to GAPDH. (*A–C*) Hippocampal mRNA expression levels of Iba-1 (*A*), TREM2 (*B*), and ADAM10 (*C*). (*D*) Concentration of sTREM2. (*E* and *F*) Activation levels of proinflammatory signaling pathways. The relative amounts of phospho-p38 (Thr180/Tyr182) to total p38 (*E*) and phospho-NF-κB p65 (Ser536) to total NF-κB p65 (*F*) were determined by Western blot and densitometry. Representative images are shown at the *Upper Left*. (*G–M*) Relationships between expression levels of TREM2 and levels of Iba-1 (*G*), ADAM10 (*H*), TNF-α (*I*), IL-6 (*J*), IL-1β (*K*), glutamate (*L*), and lipid peroxidation (*M*) in the hippocampal tissue. In *A–F*, data are expressed as mean ± SEM (control, $n = 4$; taxifolin, $n = 5$); *P* values were determined by Student's *t* test; $^*P < 0.05$; $^{**}P < 0.01$. In *G–M*, Pearson's correlation coefficients (*r*) were used to test the associations of interest.

inhibited oxidative tissue damage, as well as potentially contributing to lymphangiogenesis in the brain. These effects could protect neurons from cytotoxic mediator-induced cell death, thereby helping to prevent the development and progression of CAA and maintain cognitive function.

A remarkable characteristic of taxifolin is its amyloid-β–lowering effects in the brain (3). In our previous report, we suggested that a potential mechanism for taxifolin's promotion of amyloid-β removal from the brain was by stimulating the IPAD system (3). The present study has provided in vivo molecular evidence that taxifolin may also suppress the ApoE–ERK1/2–APP axis, the pathway responsible for amyloid-β transcription and secretion (29), thereby reducing the production of intracerebral amyloid-β. Thus, taxifolin may exhibit intracellular actions in the brain parenchyma that suppress amyloid-β production and extracellular actions that facilitate amyloid-β removal, synergistically preventing amyloid-β accumulation in the brain. Our findings also suggest that although the intracerebral levels of taxifolin may be limited by the low permeability of the BBB to taxifolin, it nevertheless effectively exhibits these actions in vivo. A previous in vitro study that taxifolin inhibited amyloid-β accumulation in an activated mouse neuroblastoma cell line expressing the human APP Swedish mutation (47) supports our notion that intracellular amyloid-β reduction is attributable to the direct action of taxifolin. Alternatively, these beneficial effects may have resulted from taxifolin-derived metabolites that crossed the BBB (4).

In addition to its promotion of amyloid-β removal potentially through stimulating IPAD, taxifolin elevated the expression levels of the lymphangiogenic factors LYVE-1 and VEGF-D. Central VEGF-D is necessary for neuronal function and cognition (48), so our findings imply that taxifolin has beneficially affected cognitive function as well as the integrity of the lymphatic vasculature. The mechanisms underlying the taxifolin-mediated up-regulation of LYVE-1 and VEGF-D remain unclear; however, a recent study reported that these factors were expressed by estrogen receptor signaling, thereby increasing skin lymphangiogenesis (49). In addition, the estrogen receptor has been reported to function as a receptor for taxifolin (50). These findings therefore suggest that taxifolin induces lymphangiogenesis through stimulating estrogen receptor signaling in the brain.

Although it is increasingly evident that TREM2-expressing microglia play detrimental roles in neurodegenerative diseases (13, 17), the pathological implications of TREM2 in CAA remain to be elucidated. In the present study, elevated TREM2 expression levels were significantly associated with the increase in inflammatory markers. Neuroinflammation can accelerate amyloidopathy (51) and cause neuronal cell death (47); our findings therefore imply the pathological significance of TREM2-expressing microglia in the pathogenesis of CAA. Furthermore, taxifolin treatment

improved the activation profiles of the proinflammatory responses, including TREM2 expression levels. Thus, TREM2-expressing microglia may be a key target for preventing and treating CAA, and taxifolin may be effective for improving microglial phenotypes.

Taxifolin treatment alleviated glutamate levels and oxidative tissue damage in the brain, which were not significantly associated with TREM2 expression levels. A previous in vitro study reported that taxifolin suppressed iNOS and COX-2 expression and attenuated nitrite production in activated microglia (47), implying the beneficial effects of taxifolin on other subtypes of microglia. These would have lower expression levels of TREM2 but may be implicated in the pathogenesis of CAA. We recently demonstrated that ω-3 polyunsaturated fatty acids (PUFAs) suppressed proinflammatory responses through SIRT1-mediated inhibition of the NF-κB pathway in activated microglia (52). Thus, cotreatment with taxifolin and ω-3 PUFAs may provide synergistic neuroprotective effects in CAA.

The molecular mechanisms that underlie the improvement of microglial phenotypes with taxifolin treatment remain unclear. When microglia are activated, the stable maladaptive cell polarization states can be induced through epigenetic modifications, which are implicated in neurodegenerative diseases (53). Furthermore, neuronal and glial cells showed DNA methylation changes, which were cell type specific and associated with AD Braak stage progression (54). Accordingly, our findings that taxifolin significantly affected the expression levels of DNMTs would imply the potential involvement of gene-specific and/or cell type-specific local epigenetic modifications in the pleiotropic effects of taxifolin. Conversely, we observed the global DNA methylation levels in the hippocampus and cortex to be similar between the taxifolin and control group mice. Oxidative stress has been implicated in DNA hypermethylation, whereas amyloid-β reduces global DNA methylation (55). Our results showed that oxidative stress as well as amyloid-β levels were elevated in the brains of Tg-SwDI mice without taxifolin; this implies a complex interplay between factors affecting DNA methylation in CAA. Future studies must address these issues including potential roles of DNA demethylation systems. Of note, the leukocytes of AD patients showed reduced levels of DNA methylation in intron 1 of TREM2 and increased expression levels of TREM2 compared with control subjects (56). Furthermore, in a mouse model of AD, TREM2-expressing myeloid cells in the brain were found to be derived from peripheral monocytes and involved in AD pathogenesis (15). Thus, orally administered taxifolin might contribute to improving the phenotypes of monocytes, thereby suppressing the intracerebral accumulation of inflammatory monocytes and microglia. Further studies are needed to elucidate these mechanisms.

There are some limitations that need to be addressed before clinical translation of the findings of this study. In the present study, 4-wk-old Tg-SwDI mice were fed a chow diet containing 3% taxifolin until sacrifice. Clinical studies are required to investigate the effective dose, timing of administration, and period of administration to prevent CAA in humans. Furthermore, it still remains unclear whether taxifolin has therapeutic effects on established CAA. Since the safety profile of taxifolin has been reported (5, 6), future studies to address these issues would be helpful for translating the research findings to clinical practice.

In conclusion, this study provided in vivo evidence that taxifolin orally administered over several months directly suppressed intracerebral amyloid-β production, proinflammatory mediator expression, and oxidative tissue damage in a mouse model of CAA. The findings suggested the pathological implications of TREM2 in the pathogenesis of CAA and the effectiveness of taxifolin in beneficially modulating TREM2-expressing microglia. Future studies to elucidate the mechanisms underlying the central and systemic effects of taxifolin and to develop taxifolin-based bioactive synthetic compounds could open up new avenues for providing preventive treatment for CAA.

Materials and Methods

Animals. All of the animal experiments were approved by the Animal Care and Use Committee of Japan's National Cerebral and Cardiovascular Center (approval 16068). The generation of a CAA model using homozygous C57BL/6J-Tg(Thy1-APPSwDutIowa)BWevn/J mice, also known as Tg-SwDI mice, and the oral administration of taxifolin were performed as described in our previous report (3). Briefly, heterozygous Tg-SwDI mice carrying the human *APP* gene with the Swedish/Dutch/Iowa triple mutation, which is expressed in neurons (57), were purchased from The Jackson Laboratory. Homozygous mice were generated by breeding these mice and were verified by backcrossing. Four-week-old male homozygous Tg-SwDI mice were randomly assigned to control or taxifolin groups and were fed either a standard chow control diet or a chow diet containing 3% taxifolin (Ametis JSC) for 7 mo for the immunohistochemical analysis and for 13 mo for the other analyses. The mice were maintained in a specific pathogen-free facility, with free access to water and diet under a 12:12 h light–dark cycle. Animal experiments and tissue sampling were performed in a blinded manner, and the subsequent immunohistochemical/biochemical experiments were conducted in an open-label fashion.

Metabolic Variables. Serum levels of glucose, free fatty acids (FFAs), and triglycerides were measured using a standard enzymatic assay or a commercially available ELISA kit according to the manufacturer's instructions: glucose, GLU-HL (Serotec); FFA, Nescauto NEFA-V2 (Alfresa Pharma); and triglycerides, Determiner C-TG (Kyowa Medex). Brain and serum levels of insulin were measured using ELISA (Morinaga Institute of Biological Science, Inc.), according to the manufacturer's instructions, with the brain tissues prepared as follows. The hippocampal and cortical tissues were separately homogenized in Tris-buffered saline (25 mM Tris and 137 mM NaCl at pH 7.6) containing protease inhibitors, with a Polytron Homogenizer (PCU-2-110; Kinematica GmbH). The homogenates were centrifuged at 12,000 × *g* for 15 min at 4 °C, and the supernatants were used in the ELISA analyses.

Immunohistochemical Analyses. The control or taxifolin group Tg-SwDI mice were anesthetized and transcardially perfused with PBS, followed by 4% paraformaldehyde. The brains were removed, embedded in paraffin, sliced into sagittal sections, and analyzed by immunohistochemistry using standard procedures (3). They were then counterstained with hematoxylin to detect total cells. The primary and species-specific secondary antibodies used in the immunohistochemistry are listed in *SI Appendix*, Table S1. To quantify the immunohistochemically positive cells of interest, two areas were randomly selected on each serial section, and the proportion of positive cells was obtained by dividing the number of positive cells by the total number of cells.

Total RNA Extraction and Quantitative RT-PCR. Total RNA was separately extracted from the hippocampus or cortex of the mice using ISOGEN (Wako Pure Chemical Industries), and first-strand cDNA was synthesized using a High-Capacity RNA-to-cDNA Kit (Applied Biosystems), according to the manufacturer's instructions. We measured the expression levels of the genes of interest by quantitative RT-PCR using Power SYBR Green PCR Master Mix (Applied Biosystems) and the StepOnePlus Real-Time PCR System (Applied Biosystems). The relative expression of each gene of interest was determined by the $2^{-\Delta\Delta Ct}$ method. The expression level of glyceraldehyde-3-phosphate dehydrogenase (GAPDH) was used as an internal control. The primer sequences were obtained from Sigma-Aldrich; these are listed in *SI Appendix*, Table S2.

Western Blot Analyses. Hippocampal and cortical tissues from the mice were separately resuspended in RIPA lysis buffer (150 mM NaCl, 25 mM Tris·HCl at pH 8.0, 1% Nonidet P-40, 10 mM NaF, and 1 mM Na_3VO_4) containing 1% protease inhibitor mixture (Sigma-Aldrich). The samples were vortexed for 5 min and centrifuged at 10,000 × *g* for 20 min at 4 °C, and the supernatants were analyzed by Western blot. The total proteins were resolved by SDS-polyacrylamide gel electrophoresis and transferred to polyvinylidene difluoride membranes. After blocking with a blocking solution (Nacalai Tesque), the membranes were incubated with primary antibodies overnight at 4 °C. The antibodies used are listed in *SI Appendix*, Table S1. The immunoreactive bands were detected with the appropriate horseradish peroxidase-conjugated secondary antibodies (GE Healthcare) using the ECL Prime Western Blotting Detection System (GE Healthcare). Gel images were

acquired using the ChemiDoc MP imaging system (Bio-Rad), and protein expression levels were quantified by measuring band intensities using ImageJ (NIH).

Quantification of Glutamate in Brain Tissue Extracts. Glutamate levels in the hippocampal and cortical tissues of the mice were measured using a Glutamate Colorimetric Assay Kit (BioVision), according to the manufacturer's instructions. The tissues were homogenized in the kit's Glutamate Assay Buffer and centrifuged at 13,000 × *g* for 10 min at 4 °C, and each supernatant was added to a 96-well plate. The kit's Reaction Mix, consisting of the Glutamate Assay Buffer, Glutamate Developer, and Glutamate Enzyme Mix, was added to each well, and the plate was incubated for 30 min at 37 °C in the dark. The color intensity was measured at 450 nm using a plate reader (2030 ARVO ×3; Perkin-Elmer Life Sciences) and normalized to the total protein concentration.

Quantification of Lipid Peroxidation in Brain Tissue Extracts. Lipid peroxidation levels in the hippocampal and cortical tissues of the mice were assessed according to the tissue malondialdehyde (MDA) levels, which were measured by the formation of 2-thiobarbituric acid reactive substances (TBARS) (35) using a Colorimetric TBARS Microplate Assay Kit (Oxford Biomedical Research), according to the manufacturer's instructions. The homogenates were mixed with the Indicator Solution (2-TBA solution) and incubated for 45 min at room temperature. The amount of free lipid peroxides was quantified by measuring the absorbance of each mixture at 540 nm using a plate reader. Each value was normalized to the total protein concentration.

Quantification of sTREM2 in Brain Tissue Extracts. sTREM2 levels in the hippocampal and cortical tissues of the mice were quantified using a Mouse TREM2/TREM-2 ELISA Kit (LifeSpan BioSciences, Inc.), according to the manufacturer's instructions. Brain tissues were homogenized in PBS with a glass homogenizer on ice and centrifuged at 5,000 × *g* for 5 min at 4 °C. Sandwich ELISA was used to quantify sTREM2 levels in the supernatants by measuring the optical density of the developed color at 450 nm using a plate reader.

DNA Methylation Analyses. Genomic DNA from the hippocampal or cortical tissue of the mice was separately purified using a Qiagen DNeasy Blood and Tissue Kit (Qiagen), after which the global DNA methylation levels were measured using a MethylFlash Global DNA Methylation (5-mC) ELISA Easy Kit (Colorimetric) (EpiGentek), according to the manufacturer's instructions. The 5-methylcytosine fraction of DNA was detected using antibodies for capture and detection. The developed color was measured at 450 nm using a plate reader, and the percentage of 5-methylcytosine was calculated using the formula described in the kit's instructions.

Statistical Analysis. Data are expressed as mean ± SEM. Means were compared between the groups by Student's *t* test. Pearson's correlation coefficient (*r*) was employed to examine the associations between TREM2 expression levels and the levels of microglial activation-related markers and cytotoxic mediators. Two-tailed $P < 0.05$ was considered significant. All statistical analyses were performed using SPSS v. 22.0 for Windows (IBM Japan, Ltd.).

ACKNOWLEDGMENTS. We thank Mr. Kazuya Muranaka at Kyoto Medical Center for his technical assistance. This work was supported in part by Grant-in-Aid for Scientific Research (C) (JSPS KAKENHI Grant JP19K11760 to T.I.), Grant-in-Aid for Young Scientists (B) (JP17K14958 to S.S.), Grant-in-Aid for Scientific Research (C) (JP19K07927 to M.T., JP19K07905 to H.Y., and JP17K09827 to T.K.) and (B) (JP18H02737 to N.S.-A.), and Grant-in-Aid for Exploratory Research (JP18K19769 to N.S.-A.), from Japan Society for the Promotion of Science (JSPS). This study was also supported in part by a grant from the Intramural Research Fund (29-6-15) for Cerebrovascular Diseases of National Cerebral and Cardiovascular Center (to S.S.), a grant from Takeda Science Foundation (to M.T.), a grant from Health Science University (to M.T.), a grant from Smoking Research Foundation (128 to N.S.-A.), and a grant from the National Hospital Organization for collaborative clinical research (H26-NHO-02 to N.S.-A.). The funders had no role in data collection, analysis, decision to publish, or preparation of the manuscript.

1. Saito S, Yamamoto Y, Ihara M (2015) Mild cognitive impairment: At the crossroad of neurodegeneration and vascular dysfunction. *Curr Alzheimer Res* 12:507–512.
2. Charidimou A, et al. (2017) Emerging concepts in sporadic cerebral amyloid angiopathy. *Brain* 140:1829–1850.
3. Saito S, et al. (2017) Taxifolin inhibits amyloid-β oligomer formation and fully restores vascular integrity and memory in cerebral amyloid angiopathy. *Acta Neuropathol Commun* 5:26.
4. Yang P, et al. (2016) Detection of 191 taxifolin metabolites and their distribution in rats using HPLC-ESI-IT-TOF-MS(n). *Molecules* 21:E1209.
5. Booth AN, Deeds F (1958) The toxicity and metabolism of dihydroquercetin. *J Am Pharm Assoc Am Pharm Assoc* 47:183–184.
6. Schauss AG, Tselyico SS, Kuznetsova VA, Yegorova I (2015) Toxicological and genotoxicity assessment of a dihydroquercetin-rich dahurian larch tree (Larix gmelinii Rupr) extract (lavitol). *Int J Toxicol* 34:162–181.
7. Delporte C, et al. (2005) Analgesic-antiinflammatory properties of Proustia pyrifolia. *J Ethnopharmacol* 99:119–124.
8. Wang YH, et al. (2006) Taxifolin ameliorates cerebral ischemia-reperfusion injury in rats through its anti-oxidative effect and modulation of NF-kappa B activation. *J Biomed Sci* 13:127–141.
9. Sato M, et al. (2013) Structure-activity relationship for (+)-taxifolin isolated from silymarin as an inhibitor of amyloid β aggregation. *Biosci Biotechnol Biochem* 77:1100–1103.
10. Sato M, et al. (2013) Site-specific inhibitory mechanism for amyloid β42 aggregation by catechol-type flavonoids targeting the Lys residues. *J Biol Chem* 288:23212–23224.
11. Saito S, Ihara M (2014) New therapeutic approaches for Alzheimer's disease and cerebral amyloid angiopathy. *Front Aging Neurosci* 6:290.
12. Yeh FL, Hansen DV, Sheng M (2017) TREM2, microglia, and neurodegenerative diseases. *Trends Mol Med* 23:512–533.
13. Jay TR, von Saucken VE, Landreth GE (2017) TREM2 in neurodegenerative diseases. *Mol Neurodegener* 12:56.
14. Kleinberger G, et al. (2014) TREM2 mutations implicated in neurodegeneration impair cell surface transport and phagocytosis. *Sci Transl Med* 6:243ra86.
15. Jay TR, et al. (2015) TREM2 deficiency eliminates TREM2+ inflammatory macrophages and ameliorates pathology in Alzheimer's disease mouse models. *J Exp Med* 212:287–295.
16. Graham LC, et al. (2016) Chronic consumption of a western diet induces robust glial activation in aging mice and in a mouse model of Alzheimer's disease. *Sci Rep* 6:21568.
17. Tanaka M, et al. (2017) A novel TREM2-mediated link between diabetes and cognitive impairment: Recent findings and future perspectives. *J Alzheimers Dis Parkinsonism* 7:380.
18. Leyns CEG, et al. (2017) TREM2 deficiency attenuates neuroinflammation and protects against neurodegeneration in a mouse model of tauopathy. *Proc Natl Acad Sci USA* 114:11524–11529.
19. Wu K, et al. (2015) TREM-2 promotes macrophage survival and lung disease after respiratory viral infection. *J Exp Med* 212:681–697.
20. Zhong L, et al. (2017) Soluble TREM2 induces inflammatory responses and enhances microglial survival. *J Exp Med* 214:597–607.
21. Suárez-Calvet M, et al. (2016) sTREM2 cerebrospinal fluid levels are a potential biomarker for microglia activity in early-stage Alzheimer's disease and associate with neuronal injury markers. *EMBO Mol Med* 8:466–476.
22. Tanaka M, et al. (2019) Serum soluble TREM2 is a potential novel biomarker of cognitive impairment in Japanese non-obese patients with diabetes. *Diabetes Metab* 45:86–89.
23. Ohara T, et al. (2019) Serum soluble triggering receptor expressed on myeloid cells 2 as a biomarker for incident dementia: The Hisayama Study. *Ann Neurol* 85:47–58.
24. Fossati S, Ghiso J, Rostagno A (2012) Insights into caspase-mediated apoptotic pathways induced by amyloid-β in cerebral microvascular endothelial cells. *Neurodegener Dis* 10:324–328.
25. Julien O, Wells JA (2017) Caspases and their substrates. *Cell Death Differ* 24:1380–1389.
26. Ramirez AI, et al. (2017) The role of microglia in retinal neurodegeneration: Alzheimer's disease, Parkinson, and glaucoma. *Front Aging Neurosci* 9:214.
27. Xu F, et al. (2007) Early-onset subicular microvascular amyloid and neuroinflammation correlate with behavioral deficits in vasculotropic mutant amyloid beta-protein precursor transgenic mice. *Neuroscience* 146:98–107.
28. Wilcock DM, et al. (2008) Progression of amyloid pathology to Alzheimer's disease pathology in an amyloid precursor protein transgenic mouse model by removal of nitric oxide synthase 2. *J Neurosci* 28:1537–1545.
29. Huang YA, Zhou B, Wernig M, Südhof TC (2017) ApoE2, ApoE3, and ApoE4 differentially stimulate APP transcription and Aβ secretion. *Cell* 168:427–441.e21.
30. Miao J, et al. (2005) Cerebral microvascular amyloid beta protein deposition induces vascular degeneration and neuroinflammation in transgenic mice expressing human vasculotropic mutant amyloid beta precursor protein. *Am J Pathol* 167:505–515.
31. Takeuchi H, Suzumura A (2014) Gap junctions and hemichannels composed of connexins: Potential therapeutic targets for neurodegenerative diseases. *Front Cell Neurosci* 8:189.
32. Parajuli B, Horiuchi H, Mizuno T, Takeuchi H, Suzumura A (2015) CCL11 enhances excitotoxic neuronal death by producing reactive oxygen species in microglia. *Glia* 63:2274–2284.
33. Park L, et al. (2014) Age-dependent neurovascular dysfunction and damage in a mouse model of cerebral amyloid angiopathy. *Stroke* 45:1815–1821.
34. Han BH, et al. (2015) Contribution of reactive oxygen species to cerebral amyloid angiopathy, vasomotor dysfunction, and microhemorrhage in aged Tg2576 mice. *Proc Natl Acad Sci USA* 112:E881–E890.
35. Kato N, Yanaka K, Nagase S, Hirayama A, Nose T (2003) The antioxidant EPC-K1 ameliorates brain injury by inhibiting lipid peroxidation in a rat model of transient focal cerebral ischaemia. *Acta Neurochir (Wien)* 145:489–493, discussion 493.

36. Corrigan F, Mander KA, Leonard AV, Vink R (2016) Neurogenic inflammation after traumatic brain injury and its potentiation of classical inflammation. *J Neuroinflammation* 13:264.
37. Louveau A, et al. (2015) Structural and functional features of central nervous system lymphatic vessels. *Nature* 523:337–341.
38. Chaitanya GV, et al. (2013) Inflammation induces neuro-lymphatic protein expression in multiple sclerosis brain neurovasculature. *J Neuroinflammation* 10:125.
39. Yu M, et al. (2015) The cooperative role of S1P3 with LYVE-1 in LMW-HA-induced lymphangiogenesis. *Exp Cell Res* 336:150–157.
40. Hetz C, Saxena S (2017) ER stress and the unfolded protein response in neurodegeneration. *Nat Rev Neurol* 13:477–491.
41. Sopova K, Gatsiou K, Stellos K, Laske C (2014) Dysregulation of neurotrophic and haematopoietic growth factors in Alzheimer's disease: From pathophysiology to novel treatment strategies. *Curr Alzheimer Res* 11:27–39.
42. Hoogland IC, Houbolt C, van Westerloo DJ, van Gool WA, van de Beek D (2015) Systemic inflammation and microglial activation: Systematic review of animal experiments. *J Neuroinflammation* 12:114.
43. Yang Y, et al. (2014) Functional roles of p38 mitogen-activated protein kinase in macrophage-mediated inflammatory responses. *Mediators Inflamm* 2014:352371.
44. Yang F, Tang E, Guan K, Wang CY (2003) IKK beta plays an essential role in the phosphorylation of RelA/p65 on serine 536 induced by lipopolysaccharide. *J Immunol* 170:5630–5635.
45. Jaenisch R, Bird A (2003) Epigenetic regulation of gene expression: How the genome integrates intrinsic and environmental signals. *Nat Genet* 33:245–254.
46. Okano M, Bell DW, Haber DA, Li E (1999) DNA methyltransferases Dnmt3a and Dnmt3b are essential for de novo methylation and mammalian development. *Cell* 99: 247–257.
47. Park SY, et al. (2016) Concurrent treatment with taxifolin and cilostazol on the lowering of β-amyloid accumulation and neurotoxicity via the suppression of P-JAK2/P-STAT3/NF-κB/BACE1 signaling pathways. *PLoS One* 11:e0168286.
48. Mauceri D, Freitag HE, Oliveira AM, Bengtson CP, Bading H (2011) Nuclear calcium-VEGFD signaling controls maintenance of dendrite arborization necessary for memory formation. *Neuron* 71:117–130.
49. Morfoisse F, et al. (2018) Lymphatic vasculature requires estrogen receptor-α signaling to protect from lymphedema. *Arterioscler Thromb Vasc Biol* 38:1346–1357.
50. Plísková M, et al. (2005) Effects of silymarin flavonolignans and synthetic silybin derivatives on estrogen and aryl hydrocarbon receptor activation. *Toxicology* 215:80–89.
51. Philippens IH, et al. (2017) Acceleration of amyloidosis by inflammation in the amyloid-beta marmoset monkey model of Alzheimer's disease. *J Alzheimers Dis* 55:101–113.
52. Inoue T, et al. (2017) Omega-3 polyunsaturated fatty acids suppress the inflammatory responses of lipopolysaccharide-stimulated mouse microglia by activating SIRT1 pathways. *Biochim Biophys Acta Mol Cell Biol Lipids* 1862:552–560.
53. Rodriguez RM, Suarez-Alvarez B, Lopez-Larrea C (2019) Therapeutic epigenetic reprogramming of trained immunity in myeloid cells. *Trends Immunol* 40:66–80.
54. Gasparoni G, et al. (2018) DNA methylation analysis on purified neurons and glia dissects age and Alzheimer's disease-specific changes in the human cortex. *Epigenetics Chromatin* 11:41.
55. Chen KL, et al. (2009) The epigenetic effects of amyloid-beta(1-40) on global DNA and neprilysin genes in murine cerebral endothelial cells. *Biochem Biophys Res Commun* 378:57–61.
56. Ozaki Y, et al. (2017) DNA methylation changes at TREM2 intron 1 and TREM2 mRNA expression in patients with Alzheimer's disease. *J Psychiatr Res* 92:74–80.
57. Davis J, et al. (2004) Early-onset and robust cerebral microvascular accumulation of amyloid beta-protein in transgenic mice expressing low levels of a vasculotropic Dutch/Iowa mutant form of amyloid beta-protein precursor. *J Biol Chem* 279:20296–20306.